

## Inward Membrane Current in *Chara inflata*: I. A Voltage- and Time-Dependent Cl<sup>-</sup> Component

S.D. Tyerman, G.P. Findlay, and G.J. Paterson

School of Biological Sciences, The Flinders University of South Australia, Bedford Park, South Australia, 5042

**Summary.** An inward current which increases in magnitude over a period of seconds is activated when the membrane of *Chara inflata* (a green alga) in a K<sup>+</sup>-conductive state is hyperpolarized by a voltage clamp. The peak current and the half-time of activation are exponentially dependent on membrane potential difference. It was found by using an external Cl<sup>-</sup> electrode that the component exponentially dependent on potential was due to an efflux of Cl<sup>-</sup>. The measured current-voltage curves and the kinetics of deactivation of the current showed that other time-dependent components contributed to the net inward current. The "punchthrough" theory of Coster (*Biophys. J.* 5:669–686, 1965) does not adequately explain the inward current since a "punchthrough potential" could not be obtained, and the inward current was distinctly time dependent. The voltage and time dependence of the inward current strongly suggests that the Cl<sup>-</sup> efflux activated by hyperpolarization is through voltage-gated channels which open more frequently as the membrane is hyperpolarized.

**Key Words** Cl<sup>-</sup> channels · ion channels · *Chara inflata* · membranes · punchthrough

### Introduction

In many types of green algal cells the membrane can be hyperpolarized to values between -200 and -250 mV in neutral pH (Smith & Walker, 1976; Findlay, 1982) and in *Chara corallina* the membrane potential difference (PD) during transients can go to -372 mV (Lucas, 1982). These very negative PD's are due to the operation of an electrogenic pump, probably the extrusion of protons from the cell (Kitasato, 1968; Spanswick, 1972) and cells showing these negative PD's have been referred to as being in the P-mode (Bisson & Walker, 1982). Recently, evidence has been presented indicating that the stoichiometry of the pump may be one proton per ATP hydrolyzed (Lucas, 1982; Beilby, 1984). This would put the reversal PD of the pump calculated from known values of cytoplasmic pH and ATP concentration at about -500 mV (Walker

& Smith, 1975). For the membrane PD to be less negative by some 300 mV from the pump reversal PD passive ion leaks must be shunting the pump.

To date, the Cl<sup>-</sup> efflux has not been considered to be of any great significance in the leak pathway since the tracer flux has been found generally to be small, about 1 to 10 nmol m<sup>-2</sup> sec<sup>-1</sup> (Hope et al., 1966; Smith & Walker, 1976) compared with the Cl<sup>-</sup> influx in the light and compared with the overall membrane conductance, a major part of which may be due to the pump itself (Spanswick, 1972). On the other hand Coster (1965) has reported a sudden avalanche of inward current due to the efflux of Cl<sup>-</sup> when the membrane was hyperpolarized to between -350 and -400 mV, PD's which are considerably less negative than the reversal PD of a one-proton ATPase and similar to the transient PD's observed by Lucas (1982). Furthermore, data from Coster and Hope (1968) show that the Cl<sup>-</sup> efflux increases by a factor of 10 when the PD is changed from -100 to -200 mV. Other possible "leak" fluxes have not been shown to increase to the extent that the Cl<sup>-</sup> efflux does when the membrane is hyperpolarized. For example the Cl<sup>-</sup> influx increases by only 1.8 times for a 100-mV hyperpolarization (Beilby & Walker, 1981). Also the Cl<sup>-</sup> efflux has been inferred to be strongly dependent on external pH (Coster, 1969) which is on a par with the pH dependence exhibited by the hyperpolarized membrane (Smith & Walker, 1976).

The possibility that the passive Cl<sup>-</sup> efflux may increase with decreasing pH was considered and rejected, by Kitasato (1968), as an explanation for the pH sensitivity of the hyperpolarized membrane and his results have been quoted as evidence that the Cl<sup>-</sup> efflux is unimportant (Spanswick, 1972). However, Kitasato examined the voltage sensitivity of the Cl<sup>-</sup> efflux by varying the external pH, a procedure which gives misleading results when the Cl<sup>-</sup> efflux is sensitive to both pH and PD. Indeed, the

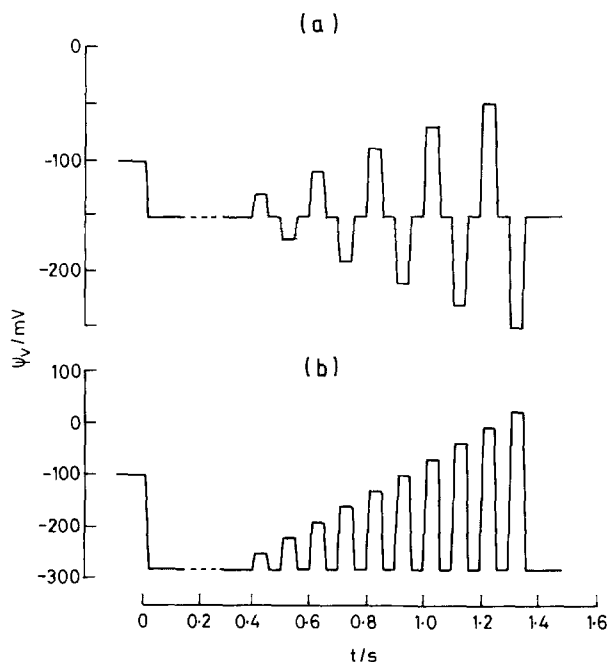


**Fig. 1.** Vacuolar potential ( $\psi_v$ ) recorded under voltage clamp as a function of time during a rapid staircase-like change in PD, a scan, which is superimposed on the main pulse. (a) Bipolar scan. (b) Unipolar positive-going scan

Cl<sup>-</sup> efflux is virtually constant in different pH when the membrane PD is free-running (Kitasato, 1968; Smith & Walker, 1976), an interesting result when one considers the large individual effects of pH and PD on the flux. These reported aspects of the Cl<sup>-</sup> efflux led us to investigate further a possible connection between the Cl<sup>-</sup> efflux and the hyperpolarized state.

We examined the inward current which flows when a membrane in a depolarized state is repolarized, using a voltage clamp, up to and beyond the levels observed in the hyperpolarized state. In this paper we report the voltage and time dependence of the inward current and attempt to identify its major ionic components. In the next paper in the series (Tyerman et al., 1985) we examine the pH dependence of the inward current and its possible connection with the hyperpolarized state. For the two studies we have chosen the whorl cells of *Chara inflata*, a close relative of *Chara corallina*, for the following reasons: (i) the cells are spherical which more easily enables isopotential voltage clamping; (ii) the membranes are easily provoked into the depolarized state. A preliminary account of this work has been given by Findlay and Tyerman (1983).

## Materials and Methods

### MATERIAL

*Chara inflata*, collected from a freshwater lake in Fairview Conservation Park, South Australia, was grown in pond water (for composition, see Coleman & Findlay, 1985) with a sandy loam sediment. The temperature was 25°C and light was provided for 12 hr per day by fluorescent tubes. The whorl cells of the plant were used for experiments. For calculating area, cells were approximated to spheres by taking the average of two orthogonal diameters (usually differing by less than 10%).

The artificial pond water (APW) bathing the experimental cells contained the following salts (concentration given in mM): KCl 1.0, NaHCO<sub>3</sub> 0.4, CaCl<sub>2</sub> 0.1, NaOH (between 0.6 and 3.4 depending on pH), zwitterionic buffer 4.0, (MES,<sup>1</sup> pH 5.0 to 6.5; HEPES,<sup>2</sup> pH 7.0 to 7.5; TAPS,<sup>3</sup> pH 8.5). Occasionally 10 mM tetraethylammonium chloride (TEACl) was added to increase the chloride concentration and to block K<sup>+</sup> channels (Armstrong, 1975).

### METHODS

#### Current and Voltage Measurements

Cells were mounted in a Perspex® holder, immobilized by being pushed into a notch by a flat-ended glass rod, illuminated by the microscope lamp and bathed in flowing solution (~1 mm/sec past cell). See Coleman and Findlay (1985) for further details.

The membrane potential difference ( $\psi$ ) was measured between a glass micropipette, filled with 3 M KCl and inserted either in the cytoplasm ( $\psi_c$ ) or in the vacuole ( $\psi_v$ ), depending on the experiment, and a reference agar-KCl salt bridge placed close to the cell in the external solution. Electrical connection from the electrodes to a unity gain differential amplifier was made through a balanced pair of calomel half-cells. The bath was held at virtual earth by a current-to-voltage amplifier. Current was injected by a Pt-Ir alloy wire, electropolished to a fine point and insulated to about 50  $\mu$ m of the tip with glass (Findlay & Hope, 1964). The sign convention is such that a movement of positive charge from outside to inside (inward current) will occur in response to  $\psi$  being clamped more negative.

When cytoplasmic recordings were attempted an electrode was first placed well into the vacuole before a second electrode was inserted. Whether the second electrode was in the cytoplasm or vacuole could be judged by the PD between the vacuolar and cytoplasmic electrodes and by the kinetics of a time- and PD-dependent K<sup>+</sup> current (Findlay & Tyerman, 1983). The time course of this current depended on whether the voltage clamp was applied to the vacuolar PD (plasmalemma and tonoplast PD's in series) or to the cytoplasmic PD (Findlay, Tyerman & Paterson, unpublished data).

<sup>1</sup> MES: (2-[N-morpholino]ethane-sulfonic acid).

<sup>2</sup> HEPES: (N-2-hydroxyethylpiperazine-N'-2-ethanesulfonic acid).

<sup>3</sup> TAPS: (tris[hydroxymethyl]methyl-aminopropanesulfonic acid).

The voltage-clamp circuit was the same as that described by Findlay and Coleman (1983) except that the command voltages were given by a computer through a Cromemco D+7A 8 bit D/A converter. Two voltage-channel outputs from the D/A were summed by a differential amplifier and low pass-filtered in order to cancel mainsline noise and reduce digital noise. A precision voltage divider resulted in the smallest increment of 2 mV over a range of 500 mV being provided to the voltage-clamp amplifier. The holding PD settled to a constant level within 20 msec of a command being made and "instantaneous" current measurements were taken routinely at 30 msec.

Voltage and current signals, amplified by 10 through buffer amplifiers were recorded by the computer every 10 msec during a pulse sequence through either a Cromemco D+7A A/D (preliminary experiments) or in most cases a Cromemco 12 bit A/D. In addition to the standard square pulses which were usually set at 12-sec duration, fast scans could be added and consisted of up to 20 sequential pulses, 50 msec long with variable amplitudes determined by software commands. Figure 1 shows the protocol of the two types of scans used; a bipolar staircase consisting of equal excursions in PD on either side of the main pulse (Fig. 1a) and a unipolar staircase consisting of only positive going steps from the main pulse (Fig. 1b). The data for each major pulse (including added scans) was stored on floppy disc and could be analyzed at a later date with the aid of a calibration data-file recorded after a run of several pulses.

### Measurements of Extracellular Chloride Concentration

In order to identify positively Cl<sup>-</sup> efflux as a component of the inward current during a hyperpolarizing step in membrane PD a Cl<sup>-</sup> electrode and a reference electrode were placed close to the cell wall, and the PD between these electrodes recorded during voltage-clamp experiments. The Cl<sup>-</sup> electrode consisted of a 0.3-mm-diameter silver wire rolled to a tip diameter of about 50 μm. The wire was encased in a glass micropipette and insulated to the tip with shellac (dissolved in methanol). The shellac coating over the end of the wire was abraded leaving a flat circular area at the tip which was chlorided using electrolysis in 0.1 M HCl. The extracellular chloride concentration was determined from the recorded PD and from a calibration curve of PD versus known concentration.

### Concentrations of Ions in the Vacuole

For measurements of the vacuolar concentrations of Na<sup>+</sup>, K<sup>+</sup> and Cl<sup>-</sup>, a sample of cells was taken from the batch used for the majority of electrical experiments. Cells were rinsed for about 30 sec in distilled water, blotted, cut open on a wax block and 10 μl of vacuolar sap withdrawn. Na<sup>+</sup> and K<sup>+</sup> concentrations were measured with an EEL flame photometer and Cl<sup>-</sup> was measured by potentiometric titration against AgNO<sub>3</sub>.

### Data Analysis

Throughout the paper, the data is presented as the median with the range and number of observations in brackets. Some kinetic

**Table.** Vacuolar concentrations and equilibrium potentials of the major ions in *Chara inflata*

Ion (mV)	Concentration (mM)	Nernst potential
Na <sup>+</sup>	92 (82, 181, <i>n</i> = 10)	-85 to -129 <sup>a</sup>
K <sup>+</sup>	83 (67, 100, <i>n</i> = 10)	-113
Cl <sup>-</sup>	137 (130, 174, <i>n</i> = 5)	121

<sup>a</sup> The range of values because of variations in [Na<sup>+</sup>]<sub>o</sub> for pH adjustment with NaOH.

data were fitted by a computer procedure using a grid search method (Bevington, 1969).

## Results

### (A) VACUOLAR ION CONCENTRATIONS

The vacuolar Na<sup>+</sup>, K<sup>+</sup> and Cl<sup>-</sup> concentrations measured in a group of cells are listed in the Table, together with the equilibrium PD for each ion calculated using the Nernst equation with external ion concentrations as in APW.

### (B) MEMBRANES IN THE K<sup>+</sup>-CONDUCTIVE STATE

Cells for which a large portion of the membrane conductance was accounted for by a time- and PD-dependent K<sup>+</sup> conductance (Coleman & Findlay, 1985) had  $\psi_o$  approximately equal to the Nernst potential for K<sup>+</sup>,  $E_K$  (Table). Cells would always enter this state by being placed in the dark. At the onset of darkness there was a transient hyperpolarization followed by a slower depolarization to  $E_K$ . The removal of external Cl<sup>-</sup> also resulted in essentially the same change in membrane PD, but slower (Tyerman et al., 1985). Occasionally a cell membrane would be in the K-state initially in the light. Unless stated otherwise the remainder of the results deals with the inward current which flows when the PD across the membrane in the K<sup>+</sup>-conductive state was stepped to more negative values by the voltage clamp.

### (C) TIME AND POTENTIAL-DEPENDENCE OF THE INWARD CURRENT

When the PD across the plasmalemma  $\psi_c$ , initially clamped at the resting level (near  $E_K$ ), was taken to a more negative level in a 12-sec pulse, the inward current was as shown in Fig. 2. In this example

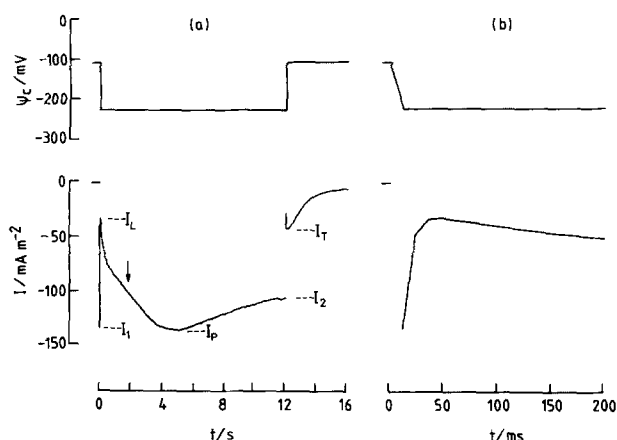


**Fig. 2.** Cytoplasmic potential ( $\psi_c$ ) (top) and inward current (bottom) as a function of time during a voltage-clamp experiment on a cell in the dark in APW pH<sub>o</sub> 6. (a) The arrow on the current trace shows the point of inflexion in the activation curve which was common to all responses. Also note the inward current tail when the potential was returned to the initial level. Various parts of the inward current have been labeled and are defined in the text. (b) Expanded scale showing the first 200 msec of the response where the decaying phase of inward current (inward-1 phase) can be seen

there is initially a very rapid decay of inward current (see first 200 msec in Fig. 2b). This current (denoted by inward-1) decayed more slowly at less negative  $\psi$  and has been attributed to the closing of K<sup>+</sup> channels (Findlay & Tyerman, 1983; Coleman & Findlay, 1985). More information on this phase of the inward current will be presented elsewhere.

After the initial decay of inward-1 current a second component appeared which increased over a period of a few seconds to a peak and then slowly declined until the end of the pulse. The increase in this inward current occurred in two phases, delimited by an inflexion in the curve (see arrow in Fig. 2a). The appearance of inward-2 current did not require the initial decay of inward-1 (K<sup>+</sup> channels shutting) since in high concentrations of KCl where the decay of inward-1 was slower, the inward-2 current would appear before the K<sup>+</sup> channels shut. Normally, the inward-1 phase had decayed before the inward-2 phase became prominent. When  $\psi_v$  was clamped and pulsed to hyperpolarized levels similar components of inward current were observed (compare Fig. 3a and 3b) but with the slow decline in the inward-2 current after the peak being less pronounced or absent.

We define various parts of the measured inward current (Fig. 2) as follows: (i)  $I_1$ , the initial current 30 msec after the start of the step in  $\psi$ ; (ii)  $I_2$ , the steady-state current, usually at 12 sec from the start

of the pulse; (iii)  $I_L$ , the minimum inward current after the inward-1 has decayed and before the inward-2 has activated; (iv)  $I_P$ , the peak value of the inward current; (v)  $I_T$ , the inward current at the peak of the current tail.

When  $\psi_c$  was returned to the initial value at the end of the pulse, a transient current (current tail) was observed (Fig. 2), which for cells in the dark always consisted of two phases, a fast initial negative-going current, sometimes beginning with outward current (see Fig. 4), followed by a slow decay back to the holding level. Cells in the light would quite often show outward current tails (for example, Fig. 13a). In cells in APW  $I_T$  was smaller than  $I_2$ . However, in high concentrations of Cl<sup>-</sup>,  $I_T$  was sometimes larger than  $I_2$  and sometimes also larger than  $I_P$ . This is illustrated in Fig. 4 for a cell in 10 mM TEACl, pH<sub>o</sub> 6.

The inward-2 current showed considerable variation between successive clamp pulses to the same  $\psi$ . Normally the current would decrease slightly with successive equally spaced pulses in time. The larger the period between pulses the smaller was the reduction of the inward-2 current. Consistent results could be obtained if pulses were separated by a constant interval of at least 10 min and before experiments, 4 or 5 test pulses to a fixed  $\psi$  were usually needed before the inward-2 current was reproducible.

Steady oscillations in the inward-2 current were observed in one cell after the addition of 1 mM nonyltriethyl ammonium bromide (C9), a K<sup>+</sup> channel blocker (Armstrong, 1975). In 0.1 mM KCl, pH<sub>o</sub> 6 the oscillations at -230 mV had an amplitude of 111 mA m<sup>-2</sup> and a period of 1.82 sec. Efforts to stimulate oscillations in other cells with C9 were not successful.

For voltage clamps of  $\psi_c$ ,  $I_L$  was small compared with the inward-2 current and we take it as an approximation to a general "leak" or nontime-dependent component of inward current. As shown in Fig. 5a, the current  $I = I_P - I_L$  could be described by an equation of the form:

$$I = -A_1 \exp(-k_1 \psi_c). \quad (1)$$

With APW pH<sub>o</sub> 6 and  $\psi_c = -300$  mV, the median value of  $I$  from Eq. (1) was -648 mA m<sup>-2</sup> (-60, -27,830,  $n = 10$ ) where  $A_1$  and  $k_1$  were  $4.66 \times 10^{-2}$  mA m<sup>-2</sup> and  $3.8 \times 10^{-2}$  mV<sup>-1</sup>, respectively. The total ranges of  $A_1$  and  $k_1$  were  $2.54 \times 10^{-4}$  to  $8.57$  mA m<sup>-2</sup> and  $1.6 \times 10^{-2}$  to  $6.2 \times 10^{-2}$  mV<sup>-1</sup>, respectively. The large value of the upper limit of the range of Eq. (1) was obtained by extrapolating the equation for a cell which had very large inward-2 currents at PD's less negative than -300 mV.

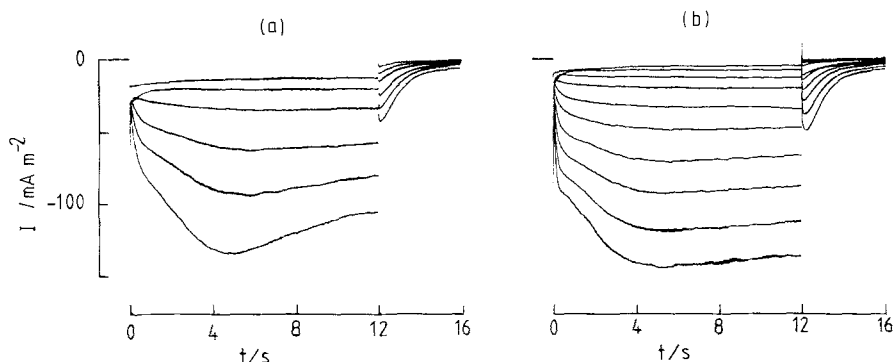


**Fig. 3.** Comparison of inward current responses as a function of time during voltage clamps of (a) cytoplasmic PD and (b) vacuolar PD for a cell in APW pH<sub>o</sub> 6. The superimposed current traces were obtained from consecutive pulses in PD incremented by 20 mV from a holding level of -108 to -228 mV in (a) and from -91 to -291 mV in (b)

The kinetics of activation of inward-2 current were also PD dependent with the time for half change to the peak ( $T_{1/2}$ ) decreasing as the PD was taken more negative (Fig. 5b). For voltage clamps of  $\psi_c$  (pH<sub>o</sub> 6)  $T_{1/2}$  could be described by the following equation:

$$T_{1/2} = A_2 \exp(k_2 \psi_c). \quad (2)$$

In APW pH<sub>o</sub> 6,  $T_{1/2}$  for  $\psi_c = -300$  mV had a median value of 0.46 sec (0.07, 0.99,  $n = 5$ ) where  $A_2$  and  $k_2$  were 40.05 sec and  $0.015 \text{ mV}^{-1}$ , respectively. The total ranges of  $A_2$  and  $k_2$  were 6.7 to 103.8 sec and  $5.4 \times 10^{-3}$  to  $24.5 \times 10^{-3} \text{ mV}^{-1}$ , respectively. For any one cell, the half-time for the decay of  $I_T$  was independent of the voltage-clamp step size. This deactivation half-time was about 0.1 to 0.6 of the extrapolated value from the activation curve (Fig. 5b).

#### (D) $I$ vs. $\psi$ CURVES

From voltage-clamp records such as those shown in Fig. 3,  $I$  vs.  $\psi$  curves can be constructed for different times during a 12-sec pulse. Figure 6 shows the effect on the shape of the  $I$  vs.  $\psi$  curves of the time at which  $I$  was sampled. The curve at 30 msec is dominated by the K<sup>+</sup> current which had not decayed, except at more negative levels of PD where a "negative resistance" region is observed. At sample times of 0.5 and 3 sec the curves are virtually linear up to about -300 mV where they start to roll over. At 12 sec, where the inward-2 current had ceased changing as a function of time, a smooth curve, exponentially dependent on  $\psi$ , is obtained.

Figure 7a shows  $I_1$  vs.  $\psi_c$  and  $I_2$  vs.  $\psi_c$  from voltage-clamp data obtained on a cell with the cytoplasmic PD clamped initially at its resting level in APW pH<sub>o</sub> 6. The  $I_1$  vs.  $\psi_c$  curve intersects the  $\psi_c$  axis at zero current (reversal PD) probably close to  $E_K$  for the cytoplasm. For small hyperpolarizations the steady-state  $I_2$  vs.  $\psi_c$  curve lies above the  $I_1$  vs.

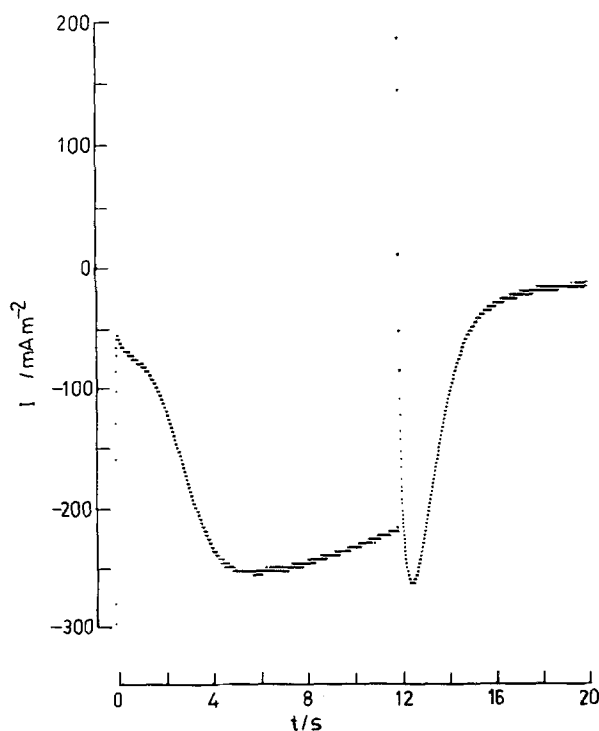


**Fig. 4.** Inward current response as a function of time when the vacuolar potential (not shown) was pulsed from -103 to -280 mV for a cell in APW pH<sub>o</sub> 6 plus 10 mM TEACl

$\psi_c$  curve illustrating the voltage- and time-dependent decrease of the K<sup>+</sup> conductance. For progressively more negative values the slope of the  $I_2$  vs.  $\psi_c$  curve increases as the inward-2 current is activated. The third curve shown in Fig. 7a is from a scan (Fig. 1) consisting of only positive-going steps in  $\psi_c$  superimposed on a negative step where the inward-2 current was large. This "instantaneous"  $I$  vs.  $\psi_c$  curve has a reversal PD at about -50 mV, less negative than  $E_K$ .

In cells in APW the  $I$  vs.  $\psi$  curves from scans were generally linear or slightly concave towards the  $\psi$  axis. For increasing values of the external

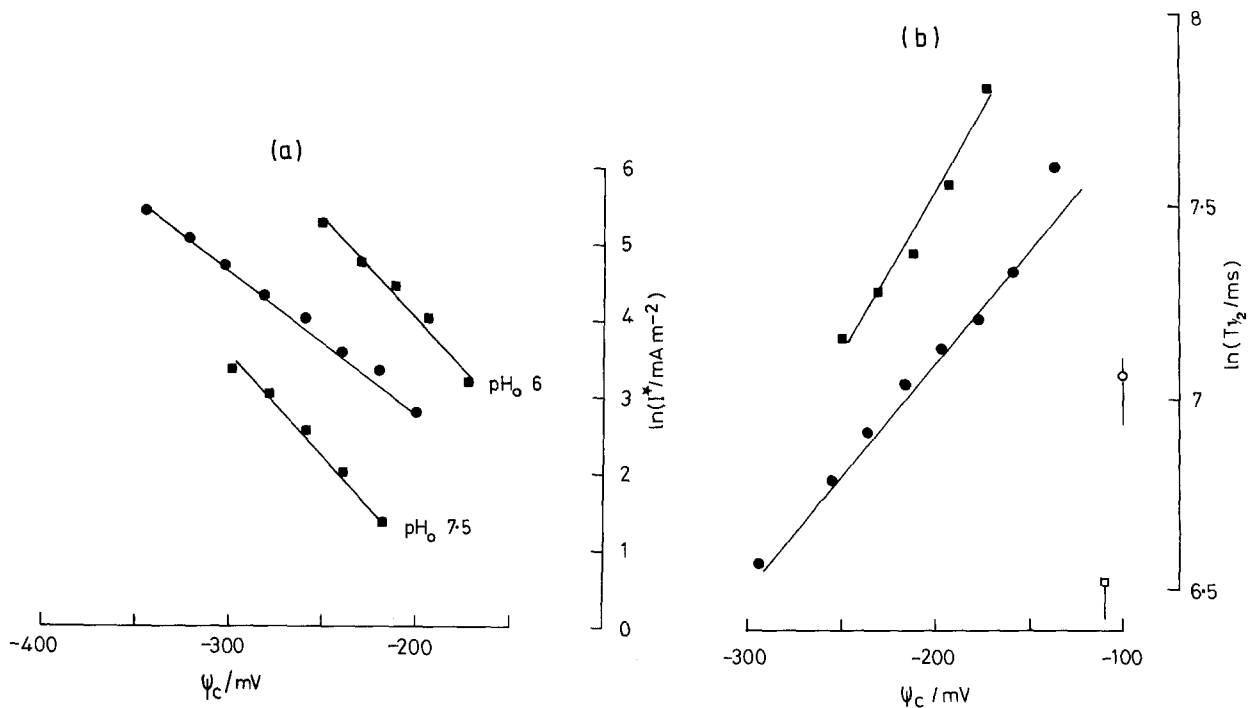


**Fig. 5.** (a) The natural logarithm of  $I^*$  vs.  $\psi_c$  for two cells under different conditions. APW  $\text{pH}_o$  6 (■),  $\text{pH}_o$  7.5 (■), and APW  $\text{pH}_o$  6 plus 10 mM KCl (●).  $I^*$  is the difference between the initial minimum inward current and the peak inward current ( $I_L - I_p$ ). (b) The natural logarithm of the time for half change ( $T_{1/2}$ ) for the activation of inward-2 current vs.  $\psi_c$  for two cells. APW  $\text{pH}_o$  6 (■), APW  $\text{pH}_o$  6 plus 10 mM KCl (●). Also shown is the median and range of  $T_{1/2}$  for the deactivation of the inward-2 current at the holding PD (open symbols)

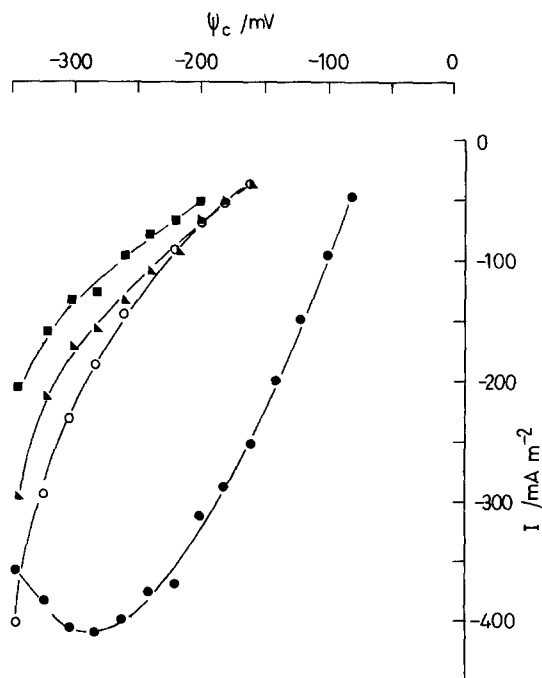


**Fig. 6.** Total inward current measured at different times into voltage-clamp pulses of  $\psi_c$ , as a function of  $\psi_c$  for a cell in APW  $\text{pH}_o$  6 + 10 mM KCl. 30 msec (●), 500 msec (■), 3 sec (▲), 12 sec (○).

concentration of  $\text{Cl}^-$ ,  $[\text{Cl}^-]_o$ , the curves became more concave towards the  $\psi$  axis suggesting at first sight that the Goldman equation may have been applicable (Jack et al., 1975). For  $[\text{Cl}^-]_o$  above about 10 mM the slope of the curves actually changed sign at PD's more negative than about  $-200$  mV. This probably indicates that because of the voltage- and time-dependent nature of the current a sample at 30 msec within each pulse of the scan was not always early enough to exclude changes in the current from the true instantaneous value; see similar results for the  $\text{K}^+$  current, shown in Fig. 6.

Figure 7b shows  $I$  vs.  $\psi$  curves for a voltage clamp of  $\psi_o$  on the same cell as shown in Fig. 7a. The resting potential of the vacuole was 30 mV more positive than that of the cytoplasm indicating a PD across the tonoplast of +30 mV (vacuole positive with respect to the cytoplasm). The  $I$  vs.  $\psi_o$  curves are similar to the  $I$  vs.  $\psi_c$  curves except for the smaller slopes of the instantaneous curves due to the addition of the tonoplast resistance and shifts in the reversal PD's to less negative values. The  $I_2$  vs.  $\psi$  curves for cytoplasm and vacuole were often almost identical for inward currents. This probably occurred because the greater driving force on the ions, responsible for the inward current in the

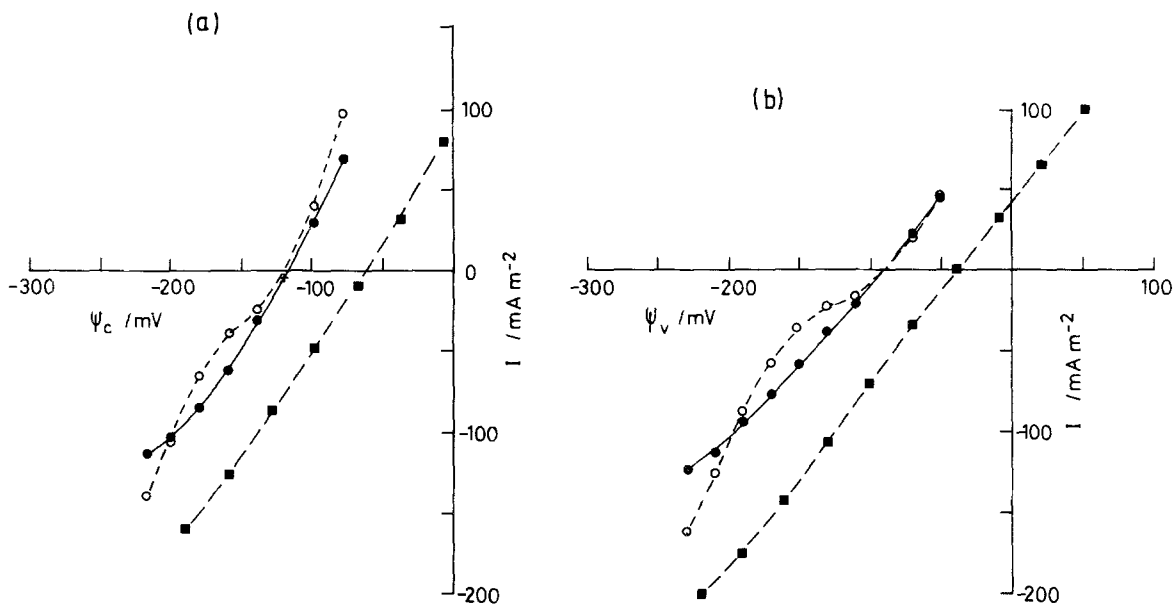


**Fig. 7.** Comparison of  $I$  vs.  $\psi$  curves between cytoplasm (a) and vacuole (b) from the same cell bathed in APW pH<sub>o</sub> 6. Currents were sampled at the standard times (see text). Initial current ( $I_1$ ) (●), final current ( $I_2$ ) (○), initial current during a scan on the inward-2 current near  $I_2$  (■)

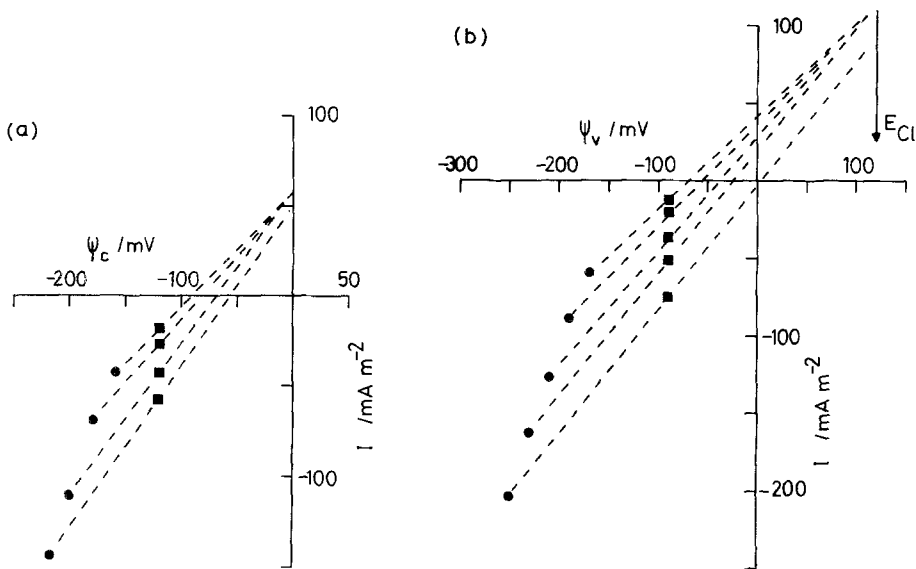


**Fig. 8.**  $I$  vs.  $\psi$  for current sampled at the end of the pulse ( $I_2$ , ●) and at the peak of the corresponding tail current ( $I_T$ , ■). Cytoplasmic curves (a) and vacuolar curves (b) for the same cell in APW pH<sub>o</sub> 6

vacuole compared with that in the cytoplasm, cancelled the effect of a slightly smaller over-all conductance between the vacuole and the outside. The tonoplast conductances of this particular cell were 2.8 S m<sup>-2</sup> with the K<sup>+</sup> conductance on and 6.45 S m<sup>-2</sup> with the inward-2 current flowing.

In an attempt to separate the components of inward-2 current we did experiments with vacuolar clamps where we applied two positive-going scans,

one before and one after the inward-2 current had turned on during the one time course. Difference  $I$  vs.  $\psi_v$  curves were then constructed and compared at different Cl<sup>-</sup> concentrations. The results were variable from cell to cell with only one out of three experiments showing results expected if Cl<sup>-</sup> carried the majority of inward-2 current. The difficulty of obtaining in the first scan an estimate of  $I_L$  undoubtedly contributed to the variability, since in the time

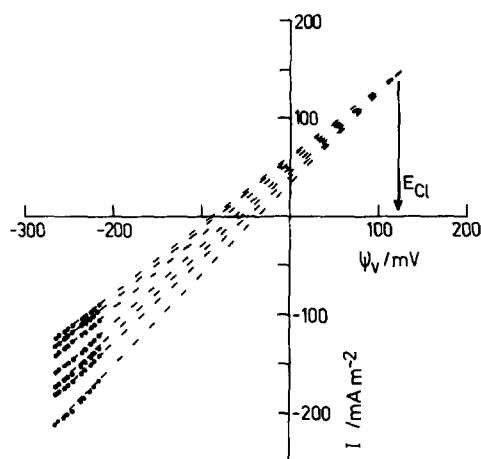


**Fig. 9.**  $I$  vs.  $\psi$  from scans performed on diminishing inward-2 current responses for consecutive pulses in  $\psi_v$  to  $-300$  mV. The extrapolated lines intersect at about  $E_{Cl}$  for the vacuole

period of one second required for the scan the current was changing significantly. In the experiment where it appeared that Cl<sup>-</sup> carried most of the inward-2 current, the reversal PD of the difference curve in 1.2 mM Cl<sup>-</sup> (pH<sub>o</sub> 5.5 and 6.0) was 125 mV. In 10.2 mM Cl<sup>-</sup> the reversal PD shifted to 31 mV and did not change significantly when K<sup>+</sup> was replaced by TEA<sup>+</sup>. When the cell was illuminated the reversal PD of the difference curves was displaced to values between  $-20$  and  $-50$  mV. A shift of the reversal PD to more negative values ( $-50$  to  $-180$ ) was obtained on illumination in the other two cells. In these cells the reversal PD in the dark was also positive (0 to 50 mV) but did not change consistently with changes in Cl<sup>-</sup> concentration. These results indicate that other ions besides Cl<sup>-</sup>, which may include a light-stimulated component, account for a variable portion of the inward-2 current.

Figure 8a shows the results from a cytoplasmic clamp where  $I_T$  and the corresponding  $I_2$  are plotted as a function of  $\psi$ . For the first three clamp pulses in which inward-2 activation occurred, a common intersection point at about 0 mV was obtained by extrapolating the lines drawn through  $I_2$  and  $I_T$ . For the fourth pulse the line did not pass through this point but was almost parallel with the line obtained from the third pulse. A vacuolar clamp on the same cell (Fig. 8b) showed that the first four pulses had a common intersection point at about  $E_{Cl}$  for the vacuole. The last pulse gave a line parallel to those from the previous pulses. At very negative potentials the reversal potential for the  $I_2$ ,  $I_T$  vs.  $\psi_v$  extrapolation was more positive than  $E_{Cl}$ . From the example shown in Fig. 4 it can be seen that the trend can continue until  $I_T$  is greater in magnitude than  $I_2$ .

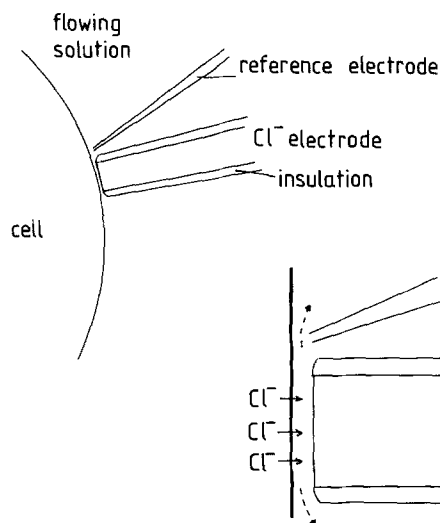


**Fig. 10.** Geometry of the Cl<sup>-</sup> electrode placement showing how small changes in local concentration were detected adjacent to the cell wall

In cells where the inward-2 current became progressively smaller during consecutive 12-sec clamp pulses to the same  $\psi_v$ , instantaneous  $I$  vs.  $\psi$  curves were obtained from scans on the inward-2 current, about 10 sec into the pulses, to shed some light on the cause of the decline of inward-2 current. An example is shown in Fig. 9. The curves show a reduction in slope and a change in the reversal PD's to more negative values corresponding to the decline of inward-2 current in successive pulses. However, the extrapolated curves all intersect at about the same PD, close to  $E_{Cl}$  for the vacuole.

#### (E) EXTRACELLULAR Cl<sup>-</sup> CONCENTRATIONS DURING THE FLOW OF INWARD-2 CURRENT

A chloride efflux was positively identified as a component of the inward-2 current in experiments using a chloride electrode and reference placed near to the cell wall. It is important to understand the geometry of the electrode placement since it is by virtue of this geometry that any Cl<sup>-</sup> could be detected at all. Figure 10 shows how the electrode itself forms the end-wall of a cylindrical segment of solution normal to the cell wall and cell membrane. Even for a small efflux of Cl<sup>-</sup> during a typical pulse, the very small volume of cylindrical segment coupled with the expected slow diffusion out through the perimeter, should allow a change in  $[Cl^-]_o$  to be detected.

Results differed from cell to cell mainly in the delay in the onset of the change in  $[Cl^-]_o$  after a change in inward-2 current flow. The length of the



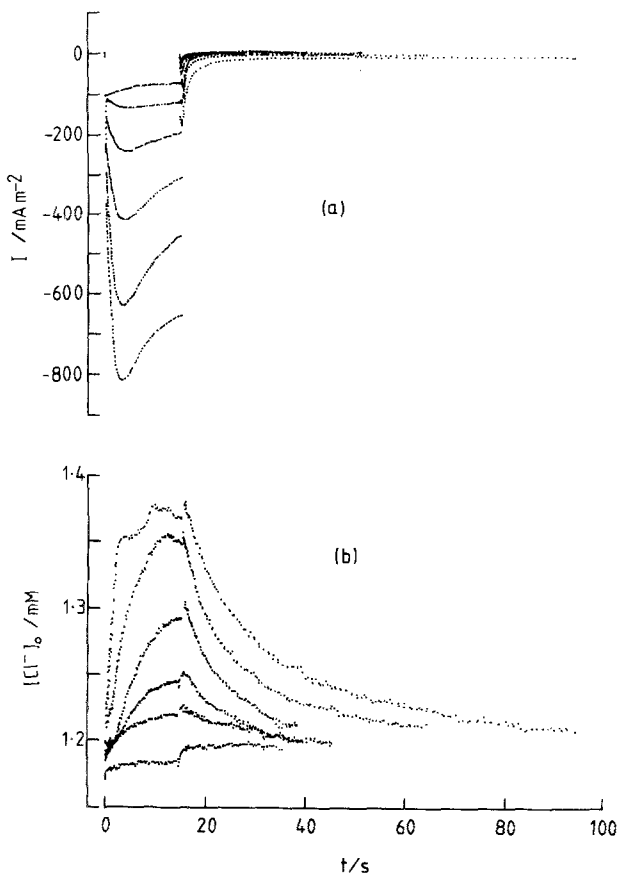


**Fig. 11.** Superimposed traces of inward-2 current (a) and the corresponding extracellular Cl<sup>-</sup> concentration (b) as functions of time for a vacuolar clamp on a cell in APW pH<sub>o</sub> 6. The PD was stepped in 50-mV increments from a holding level of -85 up to -385 mV

delay varied from cell to cell and was probably a function of the distance of the electrode from the cell wall, diffusional resistances in the wall and the magnitude of the inward-2 current. Figure 11 shows a particular example of superimposed traces of [Cl<sup>-</sup>]<sub>o</sub> as a function of time, during a sequence of negative-going voltage-clamp pulses which caused inward-2 current to flow. In this case very little delay was observed in the onset of a change in [Cl<sup>-</sup>]<sub>o</sub> and more significantly at the end of the pulse [Cl<sup>-</sup>]<sub>o</sub> had come to a steady level. From this type of response it is possible to obtain a relative measure of the Cl<sup>-</sup> efflux since the net Cl<sup>-</sup> flux across the cell membrane into the measured segment of solution must equal the net diffusional flux out of the segment into the bulk flowing solution when the concentration in the segment remains at a steady level. A flux specific to the membrane area cannot be obtained because it was not possible to obtain accurate estimates of the volume of solution being measured by the electrode. Nonetheless, relative

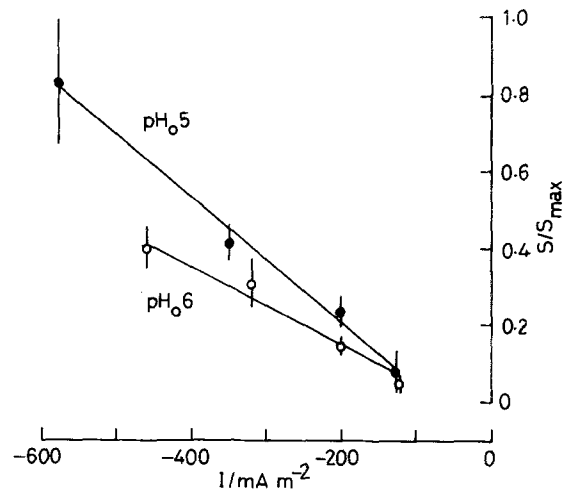


**Fig. 12.** Plot of the relative Cl<sup>-</sup> efflux ( $S/S_{\max}$ ) against the corresponding inward-2 current for a cell in pH<sub>o</sub> 5 (●) and pH<sub>o</sub> 6 (○).  $S$  is the initial slope of the decaying phase of extracellular Cl<sup>-</sup> concentration after the inward-2 current was turned off and  $S_{\max}$  is the largest slope observed within the series of responses. Error bars are estimates of the measurement errors within which  $S$  could be determined. The steps in  $\psi_v$  were the same in each pH<sub>o</sub> and were (in mV): -185, -235, -285, -335. Note that for a particular PD a larger inward-2 current was obtained in pH<sub>o</sub> 5 than in pH<sub>o</sub> 6

measures of Cl<sup>-</sup> flux can be obtained since the electrode position was constant within one experiment. During a clamp pulse, the Cl<sup>-</sup> efflux relative to a maximum observed within a sequence, was estimated from the initial rate of change in [Cl<sup>-</sup>]<sub>o</sub> when the PD was returned to the holding level, and the inward-2 current was virtually switched off. The relative flux could then be compared with the recorded inward-2 current. Figure 12 shows that for pH<sub>o</sub> 5 and 6 the ratio of Cl<sup>-</sup> efflux to the inward-2 current was a constant. In pH<sub>o</sub> 5 a larger inward-2 current was observed than in pH<sub>o</sub> 6 at the same  $\psi_v$ . This is reflected in a larger relative Cl<sup>-</sup> efflux. The effects of pH<sub>o</sub> on the inward-2 current are considered in more detail in Tyerman et al. (1986).

The ratio of Cl<sup>-</sup> efflux to inward-2 current sometimes changed with changes in external conditions at a constant  $\psi_v$ . The example in Fig. 13 shows that with the cell in the light inward-2 current was larger than that with the cell in the dark, while for the Cl<sup>-</sup> efflux the reverse was true. It is this difference in Cl<sup>-</sup> efflux, between light and dark which most likely produces the difference in direction of the current tails shown in the Figure. In the dark, with Cl<sup>-</sup> carrying the majority of the inward-2 current, the reversal PD is less negative than the holding PD of -100 mV and the tail current is negative. In the light less of the current is carried by Cl<sup>-</sup> and more appears to be carried by components with re-

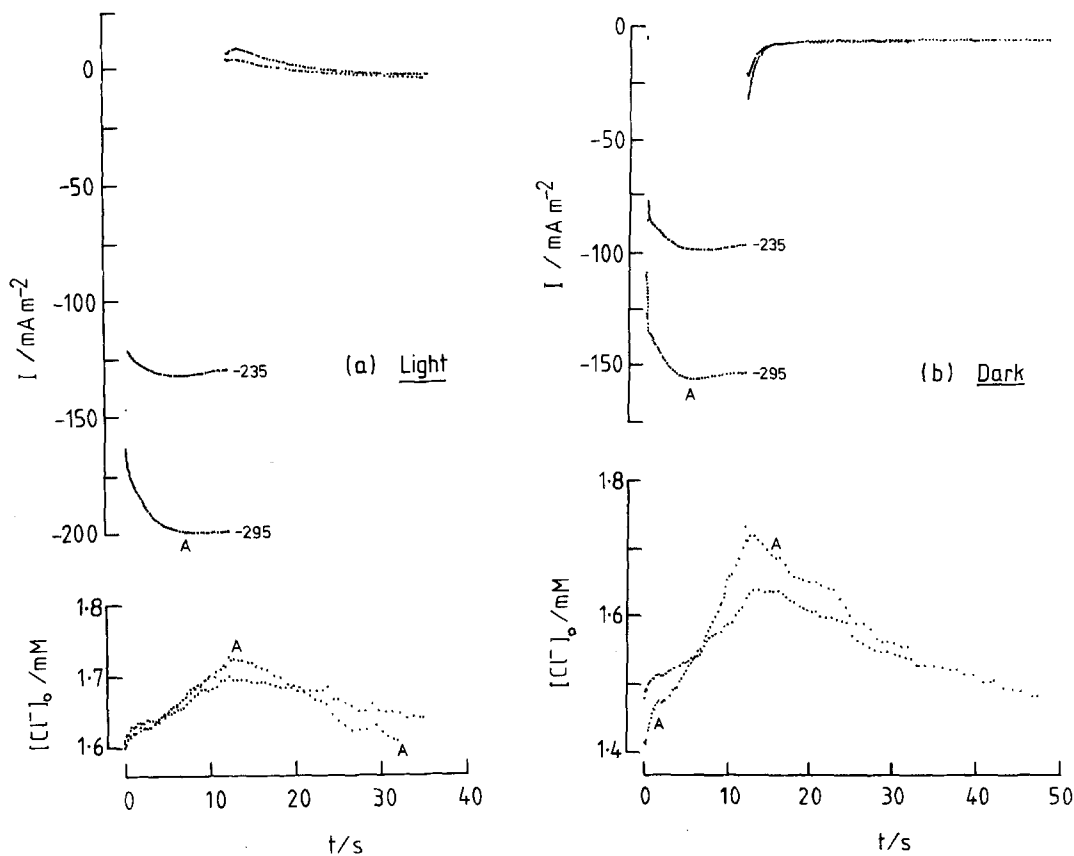


**Fig. 13.** Comparison of inward-2 current responses (top) and extracellular  $\text{Cl}^-$  responses (bottom) between light (a) and dark (b) for a cell in APW  $\text{pH}_o$  6. The levels to which  $\psi_o$  was stepped are indicated adjacent to the corresponding current trace. The letter A indicates corresponding current and  $[\text{Cl}^-]_o$  traces

versal PD's more negative than the holding PD. Thus the tail current is outwards. In cells in high  $\text{pH}_o$  less  $\text{Cl}^-$  efflux was associated with the inward-2 current than in low  $\text{pH}_o$ . An example is shown in Fig. 14. Initially, the cell was in  $\text{pH}_o$  5.5 with only a moderate amount of inward-2 current and  $\text{Cl}^-$  efflux being observed. When  $\text{pH}_o$  was changed to 8.5, no  $\text{Cl}^-$  efflux was associated with the inward-2 current (curves A), and when  $\text{pH}_o$  was changed back to 5.5, the  $\text{Cl}^-$  efflux increased in magnitude in two successive pulses (curves B and C). Atypically, the magnitude of the inward-2 current did not increase in the lower  $\text{pH}_o$ , the only indication that more  $\text{Cl}^-$  was carrying the current was the increase in magnitude of the inward current tail. Generally, in the dark the magnitudes of  $I_2$  and  $I_T$  were good indicators of the magnitude of the  $\text{Cl}^-$  efflux during the pulse.

## Discussion

### IS THE INWARD-2 CURRENT PUNCHTHROUGH?

Coster (1965) observed a sudden avalanche of inward current in *Chara corallina* at PD's of about

-300 mV. He described this phenomenon theoretically in terms of a membrane which consisted of a fixed negatively charged region on one side and a fixed positively charged region on the other. He proposed that the width of the negatively charged region ( $W_{N-}$ ) decreases more rapidly with decreasing potential than the width of the positively charged region ( $W_{N+}$ ). When  $W_{N-}$  goes to zero the anion permeability becomes very large and punchthrough occurs. In a later paper Coster (1969) showed that the phenomenon is dependent on  $\text{pH}_o$ .

For *Chara inflata* in  $\text{pH}_o$  6 for any PD we never observed a sudden cascade of inward current that could be ascribed to the punchthrough phenomenon evident at about -340 mV for *Chara corallina* in  $\text{pH}_o$  6 (Coster, 1969). Rather, the inward current was a smooth exponential function of PD (see Fig. 5a). We also found that the inward-2 current did not arise instantaneously but activated slowly over a period of seconds with complex kinetics. The time for half-change of this activation was exponentially dependent on the membrane PD (Fig. 5b). Beilby and Coster (1976) have also shown a time dependence but did not indicate that the kinetics were voltage dependent. They considered that the time

dependence did not have a significant effect on determining their punchthrough potential. However, the more sudden increase of inward current observed by Coster enabling him to obtain a punchthrough potential may only be apparent if the possible voltage dependence of the kinetics in *Chara corallina* were not taken fully into account. The effect of the time of measurement of the inward-2 current on the shape of the  $I$  vs.  $\psi_c$  curve is illustrated in Fig. 6. For currents measured between 0.5 and 3 sec into the pulse at each PD, the  $I$  vs.  $\psi_c$  curve begins to look like those presented by Coster where the curves appear almost linear up to about  $-300$  mV and then take a sudden dive. The unexpected temperature dependence of the punchthrough potential (Beilby & Coster, 1976) could be explained if decreasing temperature slowed the activation of inward-2 current, similar to the effect of temperature on the action potential (Beilby & Coster, 1979b).

“Punchthrough” has normally been regarded as a rapid avalanche of inward current accounted for by a Cl<sup>-</sup> efflux at potentials outside the normal physiological range, even though data from Coster and Hope (1968) show over a 10-fold increase in Cl<sup>-</sup> efflux between  $-100$  and  $-200$  mV. We have found for *Chara inflata* that the inward-2 current begins to activate at potentials much less negative than the levels observed in the hyperpolarized state (Tyerman et al., 1986).

#### TRANSPORT NUMBER EFFECTS

The passage of inward current under conditions which favor large concentration changes adjacent to the cell membrane will result in the electrochemical equilibrium potential of the transported ions shifting in the negative direction. Thus the observed change in the reversal PD towards positive values associated with the flow of inward-2 current, most of which is Cl<sup>-</sup>, must be due to an increase in Cl<sup>-</sup> conductance. On the other hand, the negative shift in reversal PD associated with the reduction of inward-2 current in consecutive pulses may be due to depletion of intracellular Cl<sup>-</sup>, an intracellular depletion rather than accumulation adjacent to the external membrane surface because there was sufficient time between pulses for equilibration in the external solution. For the Cl<sup>-</sup> electrode experiments some extracellular accumulation of Cl<sup>-</sup> during a pulse necessarily occurred adjacent to the cell where the electrode was placed. In most cases the concentration increased by only 0.2 to 0.4 mM which was unlikely to have had a large effect on the current.

Integration of a typical 12-sec inward-2 response at  $-300$  mV shows that a total of  $5 \times 10^{-10}$  moles of negative charge leaves the cell. If the majority of the charge were Cl<sup>-</sup> and in the worst case

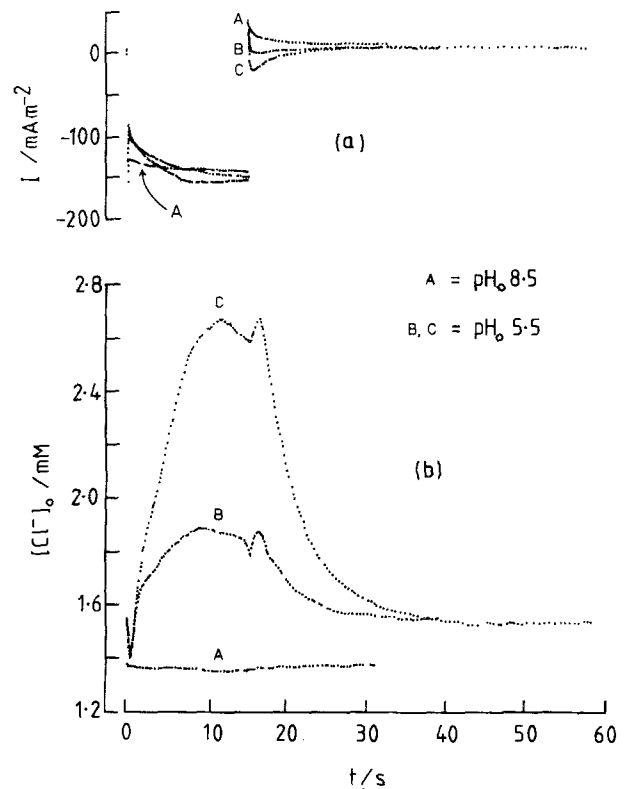


**Fig. 14.** Sequence of inward-2 current responses (a) and corresponding extracellular Cl<sup>-</sup> responses (b) when pH<sub>o</sub> was changed from 8.5 to 5.5. In each case  $\psi_v$  was pulsed to  $-300$  mV. See text for further details

there was no replenishment from the vacuole, there would be a considerable reduction in cytoplasmic Cl<sup>-</sup> during a voltage clamp of  $\psi_c$ . For example, using a cytoplasmic volume of 5% of the whole cell volume then the Cl<sup>-</sup> concentration would be reduced by about 1 mM. This is comparable to the lowest reported Cl<sup>-</sup> concentration in *Chara corallina* of 1.8 mM (Jones & Walker, 1980). The fact that longer times between pulses resulted in a smaller reduction of inward-2 current may suggest that lost Cl<sup>-</sup> could be reaccumulated from the external medium. Over a period of 10 min (the normal interval between pulses) a Cl<sup>-</sup> influx of about  $35 \text{ nmol m}^{-2} \text{ sec}^{-1}$  would replenish the amount lost during a typical inward response. This influx is large for *Chara* cells in the dark (Reid & Walker, 1984) but not impossible when compared with rates for Cl<sup>-</sup>-depleted cells (Beilby & Walker, 1981).

For voltage clamps of  $\psi_v$ , the instantaneous  $I$  vs.  $\psi_v$  curves from consecutive pulses intersected, by extrapolation, at the vacuolar  $E_{\text{Cl}}$  (Fig. 9), the reduction in inward-2 current being due to a reduction in conductance (as measured by the average slope of the lines). Thus there was no strong indication that the Cl<sup>-</sup> concentration in the vacuole was decreasing with consecutive pulses; nor would we expect it for a compartment of large volume and

high [Cl<sup>-</sup>]. Unfortunately, it was not possible to do the equivalent experiment with a cytoplasmic clamp. The intersection of the curves, shown in Figs. 8 and 9, at the vacuolar  $E_{Cl}$  also shows that the plasmalemma and tonoplast together behave as a chloride electrode plus a leak. This implies that the tonoplast, when the inward-2 current is activated, has a high Cl<sup>-</sup> conductance. If this were not the case for a vacuolar clamp, then the intersection PD would differ from the cytoplasmic  $E_{Cl}$  by the PD across the tonoplast. For cytoplasmic Cl<sup>-</sup> concentrations above about 10 mM it may become experimentally difficult to discern whether an intersection PD was indicative of the vacuolar  $E_{Cl}$  or the tonoplast PD (about 30 mV) plus cytoplasmic  $E_{Cl}$ . From our cytoplasmic data (e.g., Fig. 8) we obtained a range in cytoplasmic Cl<sup>-</sup> concentration of between 1 and 7 mM but this may have been after some depletion. We have no immediate explanation for the more obvious reduction of inward-2 current after the peak observed in cytoplasmic clamps compared with vacuolar clamps (see Fig. 3), although it is possible that an increase in tonoplast conductance, most probably to Cl<sup>-</sup> (see (D) of Results), may affect the distribution of PD across plasmalemma and tonoplast during a vacuolar clamp.

#### COMPONENTS OF THE INWARD-2 CURRENT NOT ACCOUNTED FOR BY A Cl<sup>-</sup> EFFLUX

The inward-2 current was not fully accounted for by a Cl<sup>-</sup> efflux since the reversal PD's determined from instantaneous  $I$  vs.  $\psi$  curves for inward-2 current, were more negative than  $E_{Cl}$ . The curves intersected at  $E_{Cl}$  under conditions where the Cl<sup>-</sup> component was changing at an outward current greater than about 100 mA m<sup>-2</sup>. This indicated that the component(s) accounting for the outward current at  $E_{Cl}$  had a negative reversal PD which under some conditions was more negative than  $E_K$ . Furthermore the following observations suggest that the other currents were time dependent and activated by hyperpolarizing the membrane: (i) A rapidly decreasing outward current was observed in current tails (after the capacitive spike) when  $\psi$  was returned to  $E_K$  (Fig. 4); (ii)  $I_2$ ,  $I_T$  vs.  $\psi$  curves diverged from a common intersection at  $E_{Cl}$  when the membrane was progressively hyperpolarized (Fig. 8); (iii) In high [Cl<sup>-</sup>]<sub>o</sub> peak tail currents were larger than final currents in the pulse (Fig. 4). One possible explanation of these results, in particular (iii), is that an outward current which is activated by hyperpolarization, deactivates much faster than the Cl<sup>-</sup> inward current when the membrane potential is returned from hyperpolarized levels. An equation

consisting of a constant plus the sum of two exponentials fitted tolerably well to the tail portion of the data in Fig. 4. However, the initial inward and outward currents obtained from the fit (-489 and 518 mA m<sup>-2</sup>) were very large and assuming a linear  $I$  vs.  $\psi$  curve for Cl<sup>-</sup>, the final current in the pulse  $I_2$  could not be reconstructed from the outward and inward components. Another possibility is that the large tail currents are a result of activating those Cl<sup>-</sup> channels associated with the action potential by the sudden positive-going step in PD. This possibility is also unlikely because the action potentials sometimes observed after a step back to the holding PD had quite different kinetics to the tail currents.

There are clearly other time-dependent inward currents besides that resulting from a Cl<sup>-</sup> efflux since occasionally we observed an inward-2 response without an associated Cl<sup>-</sup> flux, usually in high pH<sub>o</sub>. Normally this inward response was much smaller than those in lower pH<sub>o</sub> (Tyerman et al., 1986) where a Cl<sup>-</sup> efflux was measured. The atypical example in Fig. 14, however, shows that the non-Cl<sup>-</sup> efflux component of inward current can be large.

The initial effect of light was to stimulate the inward current but to inhibit that due to Cl<sup>-</sup> efflux. Perhaps the stimulation of inward current is indicative of the stimulating effect of light on the Cl<sup>-</sup>/2H<sup>+</sup> symporter (Sanders, 1980; Beilby & Walker, 1981). The negative shift in the reversal potential of instantaneous  $I$  vs.  $\psi$  curves could be due either to a stimulation of the outward current component (e.g. the proton pump) or inhibition of the Cl<sup>-</sup> efflux which we observed using the Cl<sup>-</sup> electrode (Fig. 13) and which has been reported from tracer experiments (Hope et al., 1966; Sanders, 1980).

#### CHLORIDE CHANNELS

Most voltage- and time-dependent macroscopic currents have now been shown to result from ion flow through discrete channels. Many are associated with membrane excitability and a common feature is that the conductance and time constant of activation are a sigmoidal and bell-shaped function of potential, respectively (Ehrenstein & Lacar, 1977). The Cl<sup>-</sup> conductance which activates by depolarization and is associated with the action-potential in *Chara corallina* shows these features (Beilby & Coster, 1979a).

In *Chara inflata* the Cl<sup>-</sup> efflux activated by hyperpolarization accounted for that part of the inward-2 current which was exponentially dependent on  $\psi_c$  and which was stimulated by lowering pH<sub>o</sub>

since the Cl<sup>-</sup> efflux was usually a constant proportion of the inward-2 current. Exceptions to this occurred soon after changes in conditions while the cell was adjusting to these changes, e.g. after the cell had been illuminated or where pH<sub>o</sub> had been changed (Fig. 14). Coster and Hope (1968) also found that the Cl<sup>-</sup> efflux calculated from radioactive tracer experiments was exponentially dependent on  $\psi$ . For *Chara inflata*, the exponential nature of the  $I_{Cl}$  vs.  $\psi$  curves means that the Cl<sup>-</sup> conductance, defined as:

$$g_{Cl} = I_{Cl}/(\psi - E_{Cl}),$$

continues to rise as  $\psi$  becomes more negative, rather than saturating to a constant value as would be observed in the two-state (open and closed) model (Jack et al., 1975; Ehrenstein & Lacar, 1977). A similar observation was made for alamethicin channels in lipid bilayers (Eisenberg et al., 1973). However, the conductance as a function of  $\psi$ ,  $g(\psi)$ , for the two-state (open and closed) model of a channel can be approximated by a single exponential function when the conductance is a small fraction of its maximum value. In this range of potentials the time constant as a function of potential is also approximated by a single exponential.

The kinetics of the macroscopic current should be first order if the two-state model of a channel were to apply. Such a model adequately describes a Cl<sup>-</sup> current in *Aplysia* neurones, a current similar to the *Chara* inward-2 current in that it is activated by hyperpolarization and is increased in magnitude as pH<sub>o</sub> is lowered (Chesnoy-Marchais, 1983). For *Chara inflata*, we could not determine whether the kinetics were first-order for the Cl<sup>-</sup> component due to the complication of at least one other time-dependent ionic current. The observed oscillations in the inward-2 current and the inductive nature of the current places it into the Model B group of ion transport systems derived by Hansen et al. (1983) which these authors state can be indicative of ion channels. Meanwhile, Coleman and Walker (1984) have used the patch-clamp technique to observe Cl<sup>-</sup> channels in *Chara corallina* which open more frequently as the membrane is hyperpolarized. These Cl<sup>-</sup> channels show more than one conductance level which may lead to an explanation for the complexity of the activation of the macroscopic current.

This project was financially supported by the Australian Research Grants Scheme. We would also like to thank Bruce White for expert technical assistance and Joseph Kourie for critically reading the manuscript.

## References

- Armstrong, C.M. 1975. Ionic pores, gates and gating currents. *Q. Rev. Biophys.* **7**:179–210
- Beilby, M.J. 1984. Current-voltage characteristics of the proton pump at *Chara* plasmalemma: I. pH dependence. *J. Membrane Biol.* **81**:113–125
- Beilby, M.J., Coster, H.G.L. 1976. Effect of temperature on punchthrough in electrical characteristics of the plasmalemma of *Chara corallina*. *Aust. J. Plant Physiol.* **3**:819–826
- Beilby, M.J., Coster, H.G.L. 1979a. The action potential in *Chara corallina*. III. The Hodgkin-Huxley parameters for the plasmalemma. *Aust. J. Plant Physiol.* **6**:337–353
- Beilby, M.J., Coster, H.G.L. 1979b. The action potential in *Chara corallina*. IV. Activation enthalpies of the Hodgkin-Huxley gates. *Aust. J. Plant Physiol.* **6**:355–365
- Beilby, M.J., Walker, N.A. 1981. Chloride transport in *Chara*. I. Kinetics and current-voltage curves for a probable proton symport. *J. Exp. Bot.* **32**:43–54
- Bevington, P. 1969. Data Reduction and Error Analysis for the Physical Sciences. McGraw-Hill, New York
- Bisson, M.A., Walker, N.A. 1982. Transitions between modes of behaviour (states) of the Charophyte plasmalemma. In: Plasmalemma and Tonoplast: Their Functions in the Plant Cell. D. Marmè, E. Marré and R. Hertel, editors. pp. 35–40. Elsevier Biomedical, Amsterdam
- Chesnoy-Marchais, D. 1983. Characterization of a chloride conductance activated by hyperpolarization in *Aplysia* neurones. *J. Physiol. (London)* **342**:277–308
- Coleman, H.A., Findlay, G.P. 1985. Ion channels in the membrane of *Chara inflata*. *J. Membrane Biol.* **83**:109–118
- Coleman, H.A., Walker, N.A. 1984. Patch clamp recording from a plant cell. Proceedings of The Australian Physiological and Pharmacological Society **15**:196
- Coster, H.G.L. 1965. A quantitative analysis of the voltage-current relationships of fixed charge membranes and the associated property of "punch-through". *Biophys. J.* **5**:669–686
- Coster, H.G.L. 1969. The role of pH in the punch-through effect in the electrical characteristics of *Chara australis*. *Aust. J. Biol. Sci.* **22**:365–374
- Coster, H.G.L., Hope, A.B. 1968. Ionic relations of cells of *Chara australis*. XI. Chloride fluxes. *Aust. J. Biol. Sci.* **21**:243–254
- Ehrenstein, G., Lacar, H. 1977. Electrically gated ionic channels in lipid bilayers. *Q. Rev. Biophys.* **10**:1–34
- Eisenberg, M., Hall, J.E., Mead, G.A. 1973. The nature of the voltage-dependent conductance induced by alamethicin in black lipid membranes. *J. Membrane Biol.* **14**:143–176
- Findlay, G.P. 1982. Electrogenic and diffusive components of the membrane of *Hydrodictyon africanum*. *J. Membrane Biol.* **68**:179–189
- Findlay, G.P., Coleman, H. 1983. Potassium channels in the membrane of *Hydrodictyon africanum*. *J. Membrane Biol.* **75**:241–251
- Findlay, G.P., Hope, A.B. 1964. Ionic relations of cells of *Chara australis* VII. The separate electrical characteristics of the plasmalemma and tonoplast. *Aust. J. Biol. Sci.* **17**:62–77
- Findlay, G.P., Tyerman, S.D. 1983. Voltage-dependent inward current in the membrane of *Chara inflata*. In: Membrane Permeability: Experiments and Models. A. Bretag, editor. Techsearch Inc., Adelaide
- Hansen, U.-P., Tittor, J., Gradmann, D. 1983. Interpretation of current-voltage relationships for "active" ion transport sys-

- tems: II. Nonsteady-state reaction kinetic analysis of class-I mechanisms with one slow time-constant. *J. Membrane Biol.* **75**:141–169
- Hope, A.B., Simpson, A., Walker, N.A. 1966. The efflux of chloride from cells of *Nitella* and *Chara*. *Aust. J. Biol. Sci.* **19**:355–362
- Jack, J.J.B., Noble, D., Tsien, R.W. 1975. Electric current flow in excitable cells. Clarendon, Oxford
- Jones, S., Walker, N.A. 1980. Chloride compartmentation in *Chara corallina* by efflux analysis. In: Plant Membrane Transport: Current Conceptual Issues. R.M. Spanswick, W.J. Lucas and J. Dainty, editors. pp. 583–584. Elsevier/North Holland Biomedical, Amsterdam
- Kitasato, H. 1968. The influence of H<sup>+</sup> on the membrane potential and ion fluxes of *Nitella*. *J. Gen. Physiol.* **52**:60–87
- Lucas, W.J. 1982. Mechanism of acquisition of exogenous bicarbonate by internodal cells of *Chara corallina*. *Planta* **156**:181–192
- Reid, R.J., Walker, N.A. 1984. The energetics of Cl<sup>-</sup> active transport in *Chara*. *J. Membrane Biol.* **78**:35–41
- Sanders, D. 1980. Control of plasma membrane Cl<sup>-</sup> fluxes in *Chara corallina* by external Cl<sup>-</sup> and light. *J. Exp. Bot.* **31**:105–118
- Smith, F.A., Walker, N.A. 1976. Chloride transport in *Chara corallina* and the electrochemical potential difference for hydrogen ions. *J. Exp. Bot.* **27**:451–459
- Spanswick, R.M. 1972. Evidence for an electrogenic ion pump in *Nitella translucens*. I. The effects of pH, K<sup>+</sup>, Na<sup>+</sup>, light and temperature on the membrane potential and resistance. *Biochim. Biophys. Acta* **288**:73–89
- Tyerman, S.D., Findlay, G.P., Paterson, G. 1985. Inward current in *Chara inflata*. II. Effects of pH, Cl<sup>-</sup>-channel blockers and NH<sub>4</sub><sup>+</sup>, and significance for the hyperpolarized state. *J. Membrane Biol.* **89**:153–161
- Walker, N.A., Smith, F.A. 1975. Intracellular pH in *Chara corallina* measured by DMO distribution. *Plant Sci. Lett.* **4**:125–132

Received 5 June 1985; revised 20 September 1985